Available online at www.sciencedirect.com
SCIENCE DIRECT®
Neuropharmacology 49 (2005) 831–842
NEURO PHARMACOLOGY
www.elsevier.com/locate/neuropharm

Ncm-D-aspartate: A novel caged D-aspartate suitable for activation of glutamate transporters and *N*-methyl-D-aspartate (NMDA) receptors in brain tissue

Yanhua H. Huang [a], Sukumaran Muralidharan [b,c], Saurabh R. Sinha [a], Joseph P.Y. Kao [b,c,*], Dwight E. Bergles [a,*]

[a] *Department of Neuroscience, Johns Hopkins University Medical School, 725 N. Wolfe Street, WBSB 813, Baltimore, MD 21205, USA*
[b] *Medical Biotechnology Center, University of Maryland Biotechnology Institute, Baltimore, MD 21201, USA*
[c] *Department of Physiology, University of Maryland School of Medicine, 725 W. Lombard Street, Baltimore, MD 21201, USA*

Received 15 April 2005; received in revised form 25 July 2005; accepted 26 July 2005

Abstract

The D-isomer of aspartate is both a substrate for glutamate transporters and an agonist of *N*-methyl-D-aspartate (NMDA) receptors. To monitor the behavior of these receptors and transporters in intact tissue we synthesized a new photo-labile analogue of D-aspartate, *N*-[(6-nitrocoumarin-7-yl)methyl]-D-aspartic acid (Ncm-D-aspartate). This compound was photolyzed rapidly ($t_{1/2}$ = 0.11 μs) by UV light with a quantum efficiency of 0.041 at pH 7.4. In acute hippocampal slices, photolysis of Ncm-D-aspartate by brief (1 ms) exposure to UV light elicited rapidly activating inward currents in astrocytes that were sensitive to inhibition by the glutamate transporter antagonist DL-*threo*-β-benzyloxyaspartic acid (TBOA). Neither Ncm-D-aspartate nor the photo-released caging group exhibited agonist or antagonist activity at glutamate transporters, and Ncm-D-aspartate did not induce transporter currents prior to photolysis. Glutamate transporter currents were also elicited in cerebellar Purkinje cells in response to photolysis of Ncm-D-aspartate. Photo-release of D-aspartate from Ncm-D-aspartate did not induce α-amino-3-hydroxy-5-methyl-4-isoxazole propionic acid (AMPA)/kainate receptor or metabotropic glutamate receptor (mGluR) currents, but triggered robust NMDA receptor currents in neurons; Ncm-D-aspartate and the photolzyed caging group were similarly inert at NMDA receptors. These results indicate that Ncm-D-aspartate can be used to study NMDA receptors at excitatory synapses and interactions between transporters and receptors in brain tissue.

Keywords: Glutamate transporter; NMDA receptor; Astrocyte; Hippocampus; GLT-1; GLAST; EAAT2; EAAT1; EAAT4

Abbreviations: NMDA, *N*-methyl-D-aspartate; AMPA, α-amino-3-hydroxy-5-methyl-4-isoxazole propionic acid; TBOA, DL-*threo*-β-benzyloxyaspartic acid; Ncm-D-aspartate, *N*-[(6-nitrocoumarin-7-yl)methyl]-D-aspartic acid; mGluRs, metabotropic glutamate receptors; MNI-L-glutamate, 4-methoxy-7-nitroindolinylglutamate; CNB, α-carboxynitrobenzyl; EAAC1, excitatory amino acid carrier 1; ACSF, artificial cerebral spinal fluid; GABA, γ-aminobutyric acid; GLAST, glutamate–aspartate transporter; EAAT4, excitatory amino acid transporter 4; GLT-1, glutamate transporter 1; LY 367385, (*S*)-(+)-α-amino-4-carboxy-2-methylbenzeneacetic acid; TEA, tetraethylammonium.

* Corresponding authors. Tel.: +1 410 955 6939; fax: +1 410 955 6942 (D.E. Bergles), Tel.: +1 410 706 4167; fax: +1 410 706 8184 (J.P.Y. Kao).
E-mail addresses: jkao@umaryland.edu (J.P.Y. Kao), dbergles@jhmi.edu (D.E. Bergles).

0028-3908/$ - see front matter © 2005 Elsevier Ltd. All rights reserved.
doi:10.1016/j.neuropharm.2005.07.018

1. Introduction

Plasma membrane glutamate transporters are required to maintain a low concentration of extracellular glutamate and to prevent excitotoxicity in the CNS. In addition to these homeostatic functions, glutamate transporters act on a rapid time scale to shape the concentration profile of glutamate at synapses, thereby regulating the spatial and temporal occupancy of receptors (Arnth-Jensen et al., 2002; Brasnjo and Otis, 2001; Carter and Regehr, 2000; Clark and Cull-Candy, 2002; Huang et al., 2004b; Oliet et al., 2001), and preserving the fidelity of transmission by limiting spillover of glutamate between neighboring synapses (Asztely et al., 1997; Diamond, 2001). Although expression of these transporters undergoes dramatic changes during development, and following brain injury and disease (Danbolt, 2001), little is known about the mechanisms responsible for regulating transporter activity under physiological conditions.

The activity of glutamate transporters can be monitored through uptake of radiolabeled substrates, through optical measurements of cytosolic pH changes or absorbance of voltage-sensitive dyes, and by recording transport-associated currents (Danbolt, 2001). Transporter current measurements provide a high fidelity, quantitative measure of glutamate uptake into individual cells (Otis and Jahr, 1998; Zerangue and Kavanaugh, 1996). To elicit transporter currents, substrates can be applied directly into the bath or through local perfusion; endogenous glutamate can be released from nerve terminals by electrical stimulation (Bergles and Jahr, 1997); or substrates can be photo-released from a caged compound (Brasnjo and Otis, 2004; Canepari et al., 2001b; Grewer et al., 2000; Huang et al., 2004b). Photolysis of caged substrates has several advantages for stimulating transporters in intact tissues: (1) it allows rapid presentation of substrates with kinetics comparable to, if not faster than, endogenous vesicular release; (2) application occurs independently of the endogenous releasing sites; and (3) responses induced by photolysis are free from mechanical artifacts and are typically more stable than those induced by pressure application. Nevertheless, few caged substrates have been developed to study transporter activity.

For a caged substrate to be suitable for physiological experiments it should be released rapidly and efficiently upon exposure to UV light, yet remain caged in solution so that the tissue is not exposed to substrate prior to photolysis. Previously developed α-carboxynitrobenzyl (CNB) caged versions of L-glutamate or D-aspartate exhibit poor stability in aqueous solutions (Grewer et al., 2001; Pettit et al., 1997), and some CNB-caged compounds exhibit antagonistic effects on NMDA receptors (Maier et al., 2005). In contrast, recently developed nitroindolyl (NI)- and methoxy-NI (MNI)-caged L-glutamate and D-aspartate are stable in physiological saline and biologically inert (Huang et al., 2005; Maier et al., 2005). The (6-nitrocoumarin-7-yl)methyl (Ncm) cage is structurally related to the 2-nitrobenzyl cage, and the mechanism underlying photochemical release of 2-nitrobenzyl-caged molecules has been studied extensively (Walker et al., 1988, 1989; Yip et al., 1985, 1991; Schupp et al., 1987; Zhu et al., 1987). The Ncm cage is based on the widely used coumarin chromophore, which is designed for improved absorption of the near-ultraviolet light (300–400 nm) commonly used in photo-release experiments. A facile synthesis starting with inexpensive commercially available reagents affords the Ncm cage in good yield, and only mild reaction conditions are required for coupling the Ncm cage to target biomolecules such as amino acid neurotransmitters.

Although L-glutamate is the primary endogenous substrate for glutamate transporters, transporter responses elicited with L-glutamate may be influenced by simultaneous effects on the multitude of glutamate receptors present. In contrast, D-aspartate is efficiently removed by glutamate transporters (Arriza et al., 1994), but it has a low affinity for AMPA receptors, kainate receptors, and mGluRs, suggesting that a caged D-aspartate may provide the ability to study transporter activity while signaling through these receptors remains intact. The efficient transport of D-aspartate may also provide advantages for studying NMDA receptors, because clearance of D-aspartate within tissue occurs rapidly, mimicking the time course of L-glutamate removal. Therefore, caged versions of D-aspartate are better suited to study the interaction of glutamate receptors and glutamate transporters in situ.

Here we describe the synthesis of a novel-caged form of D-aspartate (Ncm-D-aspartate), in which the α-amino group of D-aspartate is covalently linked to the Ncm cage, and examine photolysis-evoked responses in neurons and glial cells in acute brain slices. Ncm-D-aspartate is stable in physiological saline, is photolyzed rapidly upon exposure to UV light, and both Ncm-D-aspartate and the photolyzed caging group are physiologically inert. Photo-release of D-aspartate from Ncm-D-aspartate triggered glutamate transporter-mediated currents in astrocytes and Purkinje cells, as well as NMDA receptor currents in pyramidal neurons; however, it did not evoke AMPA/kainate or mGluR currents. Thus, Ncm-D-aspartate can be used to examine the properties of glutamate transporters and NMDA receptors in brain tissue.

2. Methods

2.1. Synthesis and characterization of Ncm-D-aspartate

2.1.1. General

Reagents and solvents of ACS grade or better were purchased from Sigma–Aldrich Corp. (St. Louis, MO),

Advanced ChemTech, Inc. (Louisville, KY), Fischer Scientific (Pittsburgh, PA), or VWR International (West Chester, PA), and were used without further purification. Proton NMR spectra were recorded on a 300-MHz spectrometer (QE-300, General Electric Co., Fairfield, CT) and were referenced to tetramethylsilane ($\delta = 0$). High-performance liquid chromatography (HPLC) was performed on a system fitted with a photodiode array detector (Model 600, Waters Corp., Milford, MA). Fast-atom bombardment (FAB) high-resolution mass spectrometry (HRMS) was performed at the analytical facility in the Department of Biochemistry at Michigan State University (East Lansing, MI).

2.1.2. *N-[(6-Nitrocoumarin-7-yl)methyl]-D-aspartic acid (Ncm-D-Asp, **1**)*

To 3 mL of DMSO, 0.40 g of 7-(bromomethyl)-6-nitrocoumarin (Muralidharan and Kao, unpublished results), 0.39 g of H-(D)Asp-(OtBu)-OtBu·HCl (Advanced ChemTech), and 0.58 mL of triethylamine were added. The mixture was stirred for 4 h at room temperature. The solvent and excess triethylamine were removed under vacuum. The residue was purified by column chromatography on silica gel (5:95, v/v CH_3CN/CH_2Cl_2) to give 0.34 g (67% yield) of *N*-[(6-nitrocoumarin-7-yl)methyl]-D-aspartic acid, di(*t*-butyl) ester (**2**) as a viscous oil. ^{1}H NMR ($CDCl_3$), δ 8.21 (s, 1H), 7.76–7.73 (m, 2H), 6.53 (d, $J = 9.5$ Hz, 1H), 4.23 (dd, AB type, $J_{AB} = 16.6$ Hz, 2H), 3.48 (t, $J = 6.3$ Hz, 1H), 2.69–2.55 (m, 2H), 1.46–1.43 (m, 18H). To remove the *t*-butyl protective groups, a solution of 0.08 g of **2** in 1 mL glacial acetic acid was maintained at ice/water bath temperature. Concentrated HBr (1 mL) was added and the stirred solution was maintained in the ice/water bath for 15 min. After removal of the acetic acid and HBr under vacuum, 1 mL of water was added to the residue. The resulting solution was purified batch wise on a semi-preparative HPLC column (Intersil 5μ ODS-3, MetaChem Technologies, Inc. Torrance, CA). The mobile phase was acetonitrile–water (containing 0.1% v/v trifluoroacetic acid). Details of the solvent profile are in Supplemental Information. The fraction eluting at 10–12 min was collected and lyophilized. The purity of the lyophilized material was again checked by HPLC. After deprotection and purification, 0.053 g of **1** was obtained from 0.08 g of **2** (yield = 89%). ^{1}H NMR [$(CD_3)_2SO$], δ 8.52 (s, 1H), 8.17 (d, $J = 9.5$ Hz, 1H), 7.79 (s, 1H), 6.64 (d, $J = 9.5$ Hz, 1H), 4.14 (dd, AB type, $J_{AB} = 16.8$ Hz, 2H), 3.47 (t, $J = 6.2$ Hz, 1H), 2.65–2.52 (m, 2H). HRMS (FAB): $C_{14}H_{13}N_2O_8$, $[M^+ + H]$ m/z, calculated, 337.0672; found, 337.0673.

2.1.3. *Quantum yield of photolysis*

A pulsed Nd:YAG laser (Quanta-Ray GCR-18S, Spectra Physics, Mountain View, CA), operating at 1 Hz, was used as the photolysis light source. The third harmonic emission (355 nm) was isolated from the fundamental (1064 nm) and second harmonic (532 nm) emissions by passing the output of the laser through 2 harmonic separators. We used a standard chemical actinometer (potassium ferrioxalate; Hatchard and Parker, 1956) to confirm that the laser output power was stable (1.4% over 2.5 h), and that energy output was linearly related to the number of laser pulses (>99.8% linearity from 1 to 60 pulses). A solution of **1** in 0.1 M sodium phosphate buffer (pH = 7.41) was prepared to have an absorbance > 2.5 at 355 nm. In all cases, we ensured that <20% of **1** was consumed by photolysis. This was confirmed by HPLC analysis using 4-nitrophenol as an internal standard: equal amounts of 4-nitrophenol were added to the photolyzed and unphotolyzed samples of **1** and the extent of consumption of **1** was determined by the integration of corresponding peaks in the HPLC (de Mayo and Shizuka, 1976). Photolysis experiments were performed in triplicate; each HPLC analysis was repeated 2 or 3 times.

2.1.4. *Kinetics of flash photolysis*

The kinetics of flash photolysis was studied on a kinetic spectrophotometer (LP920, Edinburgh Instruments, Livingston, UK). An aqueous solution of **1** in 0.1 M sodium phosphate (pH 7.41) was prepared to have absorbance > 2.0 (in a 1-cm cuvette) at 355 nm, the wavelength of the photolysis light. The air-equilibrated solution was magnetically stirred at room temperature. Photolysis of the sample was effected by an 8.6-ns (FWHM), 200 mJ pulse of 355 nm third harmonic light from a Nd–YAG laser (Quanta-Ray GCR-18S, Spectra Physics). A pair of harmonic separators was used to remove residual fundamental (1064 nm) and second harmonic (532 nm) laser emissions from the photolysis beam. A probe beam from a stabilized xenon arc lamp was focused such that the focal point coincided with the region in the sample where maximal photolysis occurred. The spectrum of the probe beam was obtained through a monochromator. Modulation of the probe beam intensity by a transient photochemical intermediate species was monitored at a chosen wavelength (430 nm in the reported experiments) by a fast photomultiplier tube. The intensity-versus-time profile was converted to an absorbance-versus-time trace. Nonlinear least-squares analysis allowed exponential decay times to be extracted from the data. Data in the initial 45-ns window contain artifactual contributions from scattering of the laser pulse and instabilities in the high-sensitivity detection circuitry, and are not included in data analysis.

2.2. *Slice preparation and electrophysiology*

Hippocampal slices were prepared from 12- to 17-day-old Sprague–Dawley rats in accordance with a protocol approved by the Animal Care and Use Committee

at Johns Hopkins University. Rats were deeply anesthetized with halothane and decapitated, the hippocampi were dissected free, mounted in agar blocks, cut into 400 μm thick transverse sections using a vibratome (VT1000S, Leica), in oxygenated ice-cold artificial cerebrospinal fluid (ACSF) containing (in mM): NaCl 119, KCl 2.5, $CaCl_2$ 2.5, $MgCl_2$ 1.3, NaH_2PO_4 1, $NaHCO_3$ 26.2 and D-Glucose 11. Slices were allowed to recover in ACSF at 37 °C for 30 min and kept at room temperature thereafter. For cerebellar slices, 250 μm thick parasagittal sections were prepared. In all cases, brain slices were used within 7 h of preparation. Brain slices that had recovered for at least 1 h were transferred to a Lucite chamber with a coverslip bottom and continuously superfused with oxygenated ACSF. Individual cells (astrocytes, Purkinje neurons or CA1 pyramidal neurons) were visualized through a 40× water immersion objective (Olympus LUMPlanFl, NA = 0.8) using an upright microscope (Axioskop FS2, Zeiss) equipped with infrared-Nomarski optics and a B&W CCD camera. Recording electrodes were pulled from glass capillary tubing and had a resistance of 1.7–3.5 MΩ when filled with the internal solution. For astrocytes, the internal solution contained (in mM): KCH_3O_3S (KMeS) 120, EGTA 10, HEPES 20, $MgCl_2$ 1, Na_2ATP 2, NaGTP 0.2; the pH was 7.3. For neuronal recordings the internal solution contained (in mM): $CsCH_3O_3S$ (CsMeS) 105, TEA-Cl 20, EGTA 10, HEPES 20, $MgCl_2$ 1, QX-314 1, Na_2ATP 2, NaGTP 0.2; the pH was 7.3. With these solutions the series resistance during recordings was <10 MΩ, and was left uncompensated. Unless stated otherwise, holding potentials have not been corrected for the junction potential. Whole-cell currents were amplified using an Axopatch 200B (Axon Instruments), filtered at 2–5 kHz and sampled at 10–20 kHz. A 0.5–5 mV hyperpolarizing step was applied at the beginning of each trace to measure both the membrane and access resistances.

2.3. Photolysis in brain slices

Caged compounds were dissolved in HEPES buffered saline (HEPES ACSF) containing (in mM): NaCl 137, KCl 2.5, $CaCl_2$ 2.5, $MgCl_2$ 1.3, HEPES 20; the pH was 7.3. Solutions containing caged compounds were applied to local regions of the slice using a wide bore (tip diameter 50–100 μm) pipette connected to a manifold fed by four 10 ml reservoirs. Valves were attached to each reservoir to control which solution the slice was exposed to. Antagonists were used to block voltage-gated Na^+ channels (tetrodotoxin; TTX, 1 μM) and NMDA receptors ((*RS*)-3-(2-carboxypiperazin-4-yl)-propyl-1-phosphonic acid; *R*,*S*-CPP, 10 μM; and (5*R*,10*S*)-(+)-5-methyl-10,11-dihydro-5*H*-dibenzo[*a*,*d*]-*cyclo*-hepten-5,10-imine hydrogen maleate; MK-801, 50 μM). For Purkinje cell experiments, antagonist to AMPA/kainate receptors (2,3-dioxo-6-nitro-1,2,3,4-tetrahydrobenzo[*f*]quinoxaline-7-sulfonamide disodium salt; NBQX, 10 μM) was included to block mEPSCs. Glutamate transporters were inhibited using DL-*threo*-β-benzyloxyaspartic acid (TBOA, 200 μM). For each experiment, the caged compound solution contained the same concentration of antagonists present in the bath solution. In some experiments, D-aspartate (500 μM dissolved in HEPES ACSF) was applied locally through a small tip pipette (~1 μm diameter) using a picospritzer (Pressure System IIe, Toohey Company); a 5–10 ms pulse of 15–20 psi was used to eject the solution. All appropriate blockers were included in the puffer pipette solution.

For photolysis, an argon ion laser (Stabilite 2017-AR, Spectra-Physics) providing ~380 mW of multi-line near UV light (333.6–363.8 nm) was coupled to the microscope through a multi-mode quartz fiber optic cable (Oz Optics Ltd.). The output of the fiber optic was collimated using a quartz lens, projected through the fluorescence port of a Zeiss Axioskop FS2 microscope, and focused to a ~50 μm spot using a 40× water immersion objective (Olympus LUMPlanFl) for recordings from astrocytes and pyramidal neurons, and to a ~100 μm spot using a 20× water immersion objective (Olympus UMPlanFl) for recordings from Purkinje cells. The UV spot was centered on the soma of astrocytes or pyramidal cells or on the dendrites of Purkinje cells, using a targeting laser (633 nm HeNe). To control the length of exposure, a computer-controlled programmable pulse generator (Master 8, AMP Instruments) was used to trigger a high-speed laser shutter (NM laser) placed between the laser head and the fiber launch. Photolysis was achieved by opening the shutter for 1 ms. In some experiments, the intensity of the laser was varied using the aperture on the laser head. The output intensity for each aperture was measured using a power meter. A laser intensity (at the output) of 380 mW was used for all other recordings, corresponding to a total light energy of 48 mJ/cm^2. This value reflects the laser power prior to entering the fiber optic; the energy reaching the cell is likely to be considerably less due to loss at the fiber launch, the microscope lenses, and the intervening tissue. MNI-L-glutamate, NBQX, *R*,*S*-CPP, MK-801, and TBOA were purchased from Tocris. D-Aspartate was purchased from Sigma. TTX and QX-314 (*N*-(2,6-dimethylphenylcarbamoylmethyl) triethylammonium chloride) were purchased from Alomone Labs.

2.4. Data analysis and statistics

Data were analyzed off-line using Clampfit (Axon Instruments) and Origin (OriginLab Corp.) softwares. For experiments on astrocytes, only cells in which the amplitude of the response to a −5 mV step changed by less

than 25% during the course of an experiment were analyzed. All values are represented as mean ± standard error of the mean. The Student's *t*-test (paired or unpaired, as appropriate) was used for statistical comparison; $P < 0.05$ was considered significant. The rise times of responses were measured from 10% to 90% of the peak amplitude, and the τ-decay was measured using a single exponential least squares fit. Half decay refers to the time required for the response to decay from 100% to 50% of the peak amplitude. For NMDA receptor currents, 90–50% decay time was measured because of the large amount of noise around the peak of the response.

3. Results

3.1. Synthesis and biophysical properties of Ncm-D-aspartate

Ncm-D-aspartate was synthesized as outlined in Fig. 1A. Details of the synthetic procedures are described in Section 2. The photochemical process through which D-aspartate is generated from Ncm-D-aspartate is shown in Fig. 1B. The UV–visible absorption spectrum of Ncm-D-aspartate, presented as extinction coefficient (ε) versus wavelength, is shown as the solid curve in Fig. 2A. As expected, the spectrum changes markedly when the sample is photolyzed with UV light (dashed curve in Fig. 2A). The quantum efficiency for photo-release of D-aspartate (Q) upon photolysis was 0.041 ± 0.005 ($n = 3$).

For studying photolysis kinetics, we used transient absorption spectroscopy to monitor the short-lived, photolytically-generated *aci*-nitro intermediate (species in brackets, Fig. 1B) (Schupp et al., 1987; Yip et al., 1985, 1991; Zhu et al., 1987), whose decay is commonly taken to be concomitant with cleavage of the caging group and release of product (McCray and Trentham, 1989; Walker et al., 1988). The kinetic spectroscopy trace for photolysis of Ncm-D-aspartate in 0.1 M sodium phosphate buffer (pH 7.41) is shown in Fig. 2B. Photolysis by a single 8.6 ns pulse of 355 nm light gave rise to a transient spectroscopic trace displaying a single-exponential time course, with exponential time constant $\tau = 158 \pm 3$ ns (equivalent to a half-life of $t_{1/2} = 110 \pm 2$ ns). That is, photo-release of D-aspartate was complete in <0.5 μs following flash photolysis. Photolysis kinetics of Ncm-D-aspartate depended strongly on solvent conditions, being fastest in aqueous solution (see Supplemental Fig. 1).

3.2. Activation of glutamate transporters in astrocytes through photolysis of Ncm-D-aspartate

Astrocytes express glutamate transporters at a high density (Lehre and Danbolt, 1998), which can be activated in brain slices through electrical stimulation of glutamatergic axons (Bergles and Jahr, 1997), or by the application of exogenous L-glutamate through pressure or photolysis (Bergles and Jahr, 1997; Huang et al., 2004b). To determine whether photolysis of Ncm-D-aspartate induces transporter activity in this semi-intact

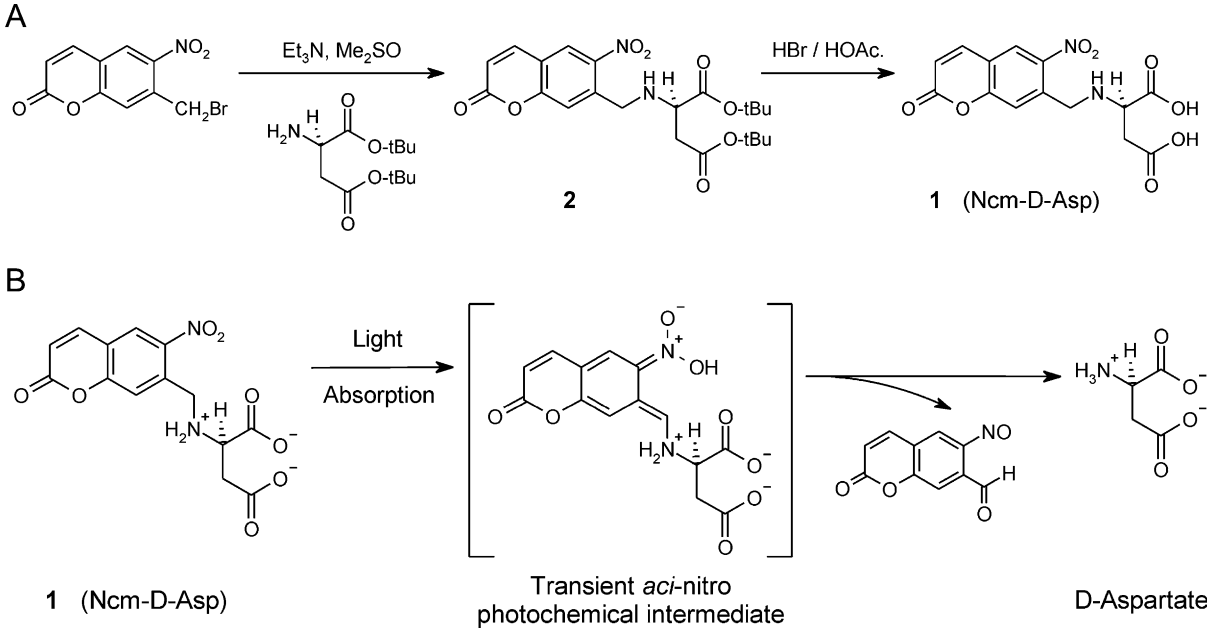

Fig. 1. Synthesis and photochemical release mechanism of Ncm-D-aspartate. (A) Synthesis and structure of *N*-Ncm-D-aspartic acid (Ncm-D-Asp). (B) Photo-release of D-aspartate from Ncm-D-aspartate. Light absorption by Ncm-D-aspartate generates the short-lived *aci*-nitro intermediate, which decomposes into the spent cage (6-nitroso-7-coumaraldehyde) and free D-aspartate.

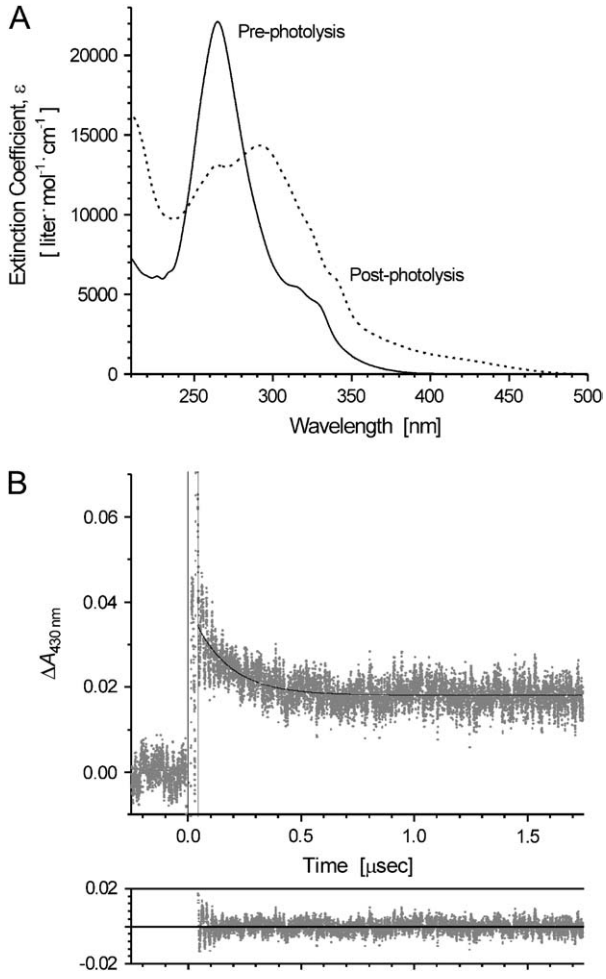

Fig. 2. Photolysis of Ncm-D-aspartate monitored by UV–visible absorption spectrum. (A) The UV–visible absorption spectra, shown in solid and dashed lines respectively, were acquired before and after photolysis of Ncm-D-aspartate for 60 s with 375 mW of the UV emission from an argon ion laser. Solvent was 0.1 M sodium phosphate buffer, pH 7.41. Extinction coefficient (ε) values are reported to facilitate readout of ε at any wavelength. (B) Photolysis kinetics measured by transient absorbance spectral change following laser flash photolysis of Ncm-D-aspartate. The absorbance at 430 nm of a solution of Ncm-D-aspartate in 0.1 M sodium phosphate (pH 7.41) was monitored. At time zero, an 8.6 ns, 200 mJ pulse of 355 nm light was delivered to the sample. In the upper panel, gray points are experimental data (average of 5 replicates), and the solid black curve is the nonlinear least-squares single-exponential fit to the data. The double vertical lines in the upper panel delimit the 45 ns window during which light scattering from the laser pulse and electronic instabilities of the photometric system contribute artifacts to the data; data within this window were not included in the least-squares analysis. The exponential time constant of the fitted decay curve is $\tau = 158 \pm 3$ ns. The residuals of the fit are shown in the lower panel. Under flash photolysis conditions, photorelease of D-aspartate is complete in <0.5 μs.

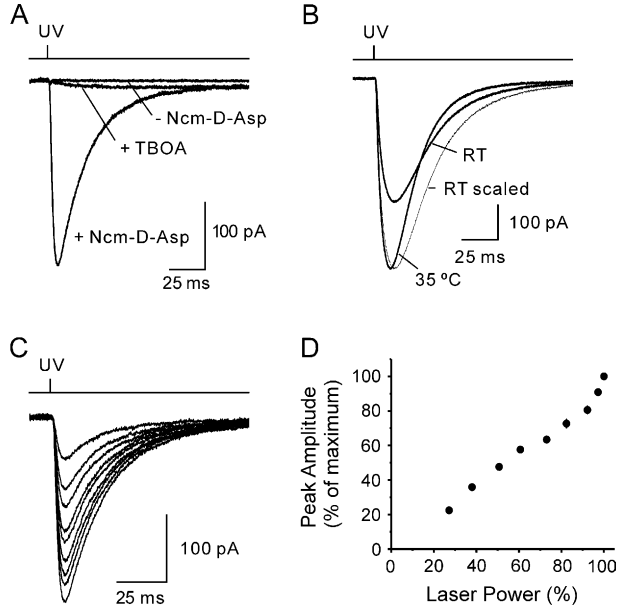

Fig. 3. Photolysis of Ncm-D-aspartate activates glutamate transporter currents in hippocampal astrocytes. (A) A transient inward current was elicited in an astrocyte by a 1 ms flash of UV laser light. The inward current was observed in the presence but not in the absence of Ncm-D-aspartate (Ncm-D-Asp, 1 mM); and was inhibited by TBOA (200 μM). The trace above shows the duration of UV exposure. (B) Glutamate transporter currents evoked in astrocytes by photolysis of Ncm-D-aspartate at room temperature (RT, 22–24 °C) and at 35 °C. The response recorded at room temperature was scaled (thin trace) to the peak of response recorded at 35 °C. (C) Glutamate transporter currents induced in a single hippocampal astrocyte by uncaging Ncm-D-aspartate (1 mM) using a range of UV light intensities. (D) Grouped data showing the relationship between light intensity and the normalized peak amplitude of the glutamate transporter current ($n = 7$). Error bars are contained within the points. All recordings were made from astrocytes located in stratum radiatum of area CA1 in the presence of TTX (1 μM), *R*,*S*-CPP (10 μM) and MK-801 (50 μM). Astrocytes were voltage-clamped at −80 mV with a KMeS-based internal solution.

preparation, we made whole-cell voltage-clamp recordings from astrocytes in the CA1 region of hippocampus and measured their response to photolysis of Ncm-D-aspartate. When the superfusing solution contained Ncm-D-aspartate (1 mM), a transient inward current was recorded from astrocytes upon brief exposure to UV light (Fig. 3A). Because D-aspartate is an agonist of NMDA receptors (Olverman et al., 1988), and astrocytes depolarize in response to changes in extracellular K^+, these responses were recorded in the presence of NMDA receptor antagonists and TTX to block the excitation of surrounding neurons (see Section 2). The currents recorded from astrocytes in response to photolysis of Ncm-D-aspartate exhibited a 10–90% rise time of 2.9 ± 0.1 ms and a decay τ of 23.3 ± 1.2 ms ($n = 7$), similar to transporter currents elicited by endogenous release from glutamatergic nerve terminals (Bergles and Jahr, 1997). The peak amplitude of these responses was 384.2 ± 56.7 pA, and was reduced by $93.9 \pm 0.6\%$ ($n = 7$) by TBOA (200 μM), a selective antagonist of glutamate transporters (Shigeri et al., 2001; Shimamoto et al., 1998) (Fig. 3A). These responses were recorded with an internal anion (MeS) that does not permeate

the glutamate transporter-associated anion channel (Bergles et al., 2002), indicating that they reflect the movement of charges that are directly coupled to the flux of D-aspartate. Following 1 ms flash of UV light, an average charge transfer of 15.8 ± 2.8 pC ($n = 7$) was elicited in astrocytes, corresponding to an uptake of 4.9×10^7 D-aspartate molecules, as two positive charges are transferred with each molecule of D-aspartate (Zerangue and Kavanaugh, 1996; Arriza et al., 1994). Moreover, if it were assumed that each transporter completes only one cycle following photolysis, an equivalent number of transporters would be activated. The total number of glutamate transporters at the astrocyte membrane is conceivably much greater, because glutamate transporters were still far from saturation under the conditions used for these experiments (see below), and there is considerable current loss across the low resistance astrocyte membrane (Bergles and Jahr, 1997). Increasing the temperature from room temperature (22–24 °C) to near physiological temperature (34–36 °C) increased the amplitude of these currents and shortened both their rise and decay times (Fig. 3B), indicating that D-aspartate is cleared more rapidly from within the slice when the cycle time of these transporters is decreased at higher temperature (Bergles and Jahr, 1998; Wadiche et al., 1995). Although the Q_{10} of steady-state cycling of EAAT2 is ~3 (Grunewald and Kanner, 1995; Wadiche et al., 1995), the charge movements observed here are likely to be dominated by the initial steps in the transport cycle, which exhibit a lower Q_{10} (Bergles and Jahr, 1998). These results indicate that UV photolysis of Ncm-D-aspartate releases D-aspartate that is subsequently removed by glutamate transporters in astrocyte membranes.

The amount of D-aspartate released by photolysis was dependent on the intensity of UV light. As shown in Fig. 3C and D, the peak amplitude of astrocyte transporter currents varied monotonically over a wide range of laser intensities ($n = 7$), indicating that the pool of transporters expressed by individual astrocytes was not saturated by the amount of D-aspartate released. The rise times of glutamate transporter currents became faster as the laser intensity was increased (10–90% rise time decreased by 8.9 ± 1.9% as relative laser power increased from 50% to 100%; $n = 7$, $P < 0.01$), similar to transporter currents recorded in outside-out patches, presumably reflecting the dependence of binding on the concentration of substrate. Although transporter currents became slightly more prolonged as the relative laser power was increased from 50% to 100% (decay τ increased by 6.2 ± 2.8%, $n = 7$), this did not reach statistical significance ($P = 0.052$). These data may indicate that the clearance of D-aspartate within the tissue becomes slower as more D-aspartate is released. However, astrocytes at this age express two distinct glutamate transporter isoforms, GLT-1 and GLAST (Huang et al., 2004b; Lehre et al., 1995; Rothstein et al., 1994). Because GLAST exhibits a lower affinity for D-aspartate and transports D-aspartate more slowly than GLT-1 (Arriza et al., 1994), it is also possible that the slowing of transporter currents at higher UV intensities arises from the recruitment of GLAST.

3.3. Physiological properties of Ncm-D-aspartate

Caged analogues of neurotransmitters are of limited value if they exhibit agonist or antagonist effects at their respective receptors, as they will alter the properties or number of receptors available prior to photolysis. Prior studies have reported that some caged compounds retain binding activity, in particular, MNI-caged-GABA and -glycine inhibit the binding of endogenous ligands to their respective receptors (Canepari et al., 2001a). To determine whether this caged form of D-aspartate is a substrate for glutamate transporters, we measured the response of astrocytes to a high concentration of Ncm-D-aspartate in the absence of UV light. Although bath perfusion of free D-aspartate (500 μM) induced an inward current of -135 ± 41 pA ($n = 4$), application of 1 mM Ncm-D-aspartate did not elicit an inward current (5.1 ± 7.9 pA, $n = 4$), indicating that this caged form of D-aspartate is not a substrate for glutamate transporters. To determine whether Ncm-D-aspartate is an antagonist of glutamate transporters we examined its effect on transporter currents evoked through local pressure application of D-aspartate (500 μM). As shown in Fig. 4A and B, application of Ncm-D-aspartate (1 mM) had little effect on the amplitude ($P = 0.786$), charge transfer ($P = 0.092$), or rise ($P = 0.188$) and decay times ($P = 0.330$) of transporter currents induced by D-aspartate, indicating that the caged compound is also not an antagonist of glutamate transporters ($n = 9$). To test whether the caging group released as a byproduct of photolysis interferes with the transport process, we examined puffer-evoked responses to D-aspartate (500 μM) in the absence and presence of the photolyzed Ncm caging group. In order to generate photolyzed Ncm cage within the tissue without concomitant release of D-aspartate, we photolyzed Ncm-glycine, a compound which shares the same caging group as Ncm-D-aspartate. The light-absorbing characteristics and quantum efficiencies of Ncm-glycine and Ncm-D-aspartate are essentially identical. As shown in Fig. 4C and D, photolysis of Ncm-glycine (1 mM) during the focal application of D-aspartate did not significantly change the amplitude ($P = 0.484$), charge transfer ($P = 0.286$), or rise ($P = 0.253$) and decay times ($P = 0.095$) of transporter currents ($n = 5$), indicating that the spent caging group also does not interfere with glutamate transport.

For a caged compound to be suitable for studying high affinity receptors such as transporters (Arriza et al., 1994) it is also important that it is stable in

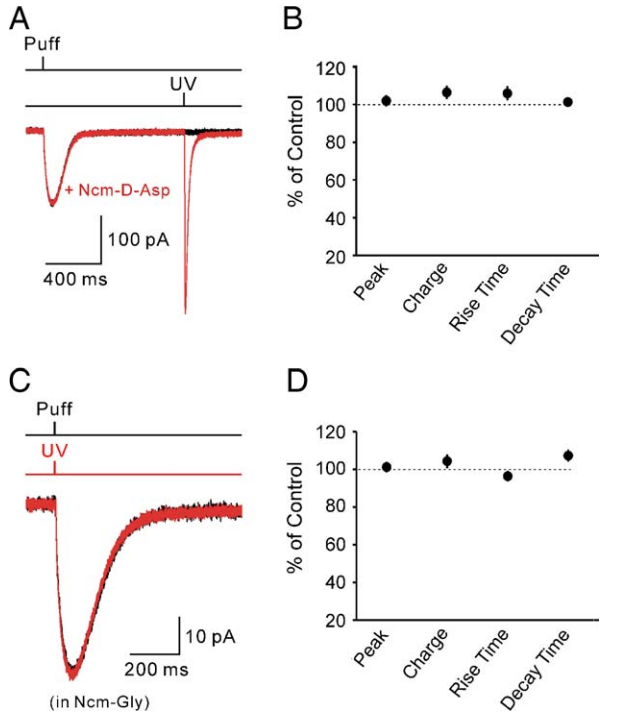

Fig. 4. Neither Ncm-D-aspartate nor the photolyzed Ncm cage antagonize glutamate transporters. (A) Glutamate transporter currents evoked in a hippocampal astrocyte by local pressure application of D-aspartate (500 μM; 5 ms pressure pulse), in the absence (black trace) and presence (red trace) of Ncm-D-aspartate (Ncm-D-Asp, 500 μM). A 1 ms UV flash was applied at the end of the recording to demonstrate the presence of the caged compound. (B) Grouped data showing the change in peak amplitude, charge transfer, 10–90% rise time and half decay time of transporter currents elicited through pressure application of D-aspartate recorded in the absence and presence of Ncm-D-aspartate (1 mM, $n = 9$). (C) Glutamate transporter currents evoked in a hippocampal astrocyte by local pressure application of D-aspartate (500 μM; 5 ms pressure pulse) recorded under control conditions (black trace) or following photolysis of 1 mM Ncm-glycine (red trace). (D) Grouped data showing the change in peak amplitude, charge transfer, 10–90% rise time and half decay time of puffer-evoked transporter currents recorded in the absence and presence of the Ncm caging group ($n = 6$). All recordings were made from astrocytes located in stratum radiatum of area CA1, in the presence of TTX (1 μM), *R,S*-CPP (10 μM) and MK-801 (50 μM). Astrocytes were voltage-clamped at −80 mV with a KMeS-based internal solution.

aqueous solutions; otherwise, a proportion of the transporter population will be occupied prior to exposure to UV light. Thermal instability is common to carboxylic acids caged by esterification with the CNB chromophore (Grewer et al., 2001; Maier et al., 2005; Pettit et al., 1997). To assess the stability of Ncm-D-aspartate, a 1 mM solution of the caged compound was prepared in HEPES ACSF (pH 7.3), stored at 4 °C in the dark, and applied to astrocytes by local perfusion 2 and 4 days later. This solution produced a change in holding current of 15.0 ± 19.9 pA ($n = 5$) at 2 days and −5.0 ± 7.5 pA ($n = 8$) at 4 days, indicating that this compound is highly stable in aqueous physiological buffer.

3.4. Glutamate transporter currents evoked in Purkinje cells through photolysis of Ncm-D-aspartate

The results described above indicate that UV photolysis of Ncm-D-aspartate yields a quantity of D-aspartate sufficient to induce cycling of large numbers of glutamate transporters in astrocytes. To determine whether this compound is also capable of inducing glutamate transporter activity in neurons, where transporters are typically expressed at a much lower density (Lehre and Danbolt, 1998), we recorded photolysis-evoked transporter currents from cerebellar Purkinje cells. These neurons express EAAT4, a transporter that exhibits a 10-fold higher affinity for glutamate than other glutamate transporter isoforms (Fairman et al., 1995), but cycles ~ 3 times more slowly than GLT-1 (Bergles and Jahr, 1998; Otis and Jahr, 1998; Auger and Attwell, 2000). Previous studies have shown that EAAT4-mediated currents can be induced in Purkinje cells following stimulation of glutamatergic parallel and climbing fiber axons (Delaney and Jahr, 2002; Otis et al., 1997), or through photolysis of CNB- (Brasnjo and Otis, 2004) or NI-L-glutamate (Canepari et al., 2001b). When UV illumination (~100 μm diameter spot) was centered in the molecular layer over Purkinje cell dendrites, an inward current of −55.3 ± 9.9 pA ($n = 5$) was elicited following a 1 ms exposure to UV light in Ncm-D-aspartate (1 mM) (Fig. 5A) that was inhibited by 86.3 ± 1.5% ($n = 5$) of 200 μM TBOA. Photolysis of Ncm-D-aspartate led to an average charge transfer of 9.6 ± 2.7 pC. If it is assumed that each EAAT4 transporter completes one cycle of transport and contributes a net influx of 2

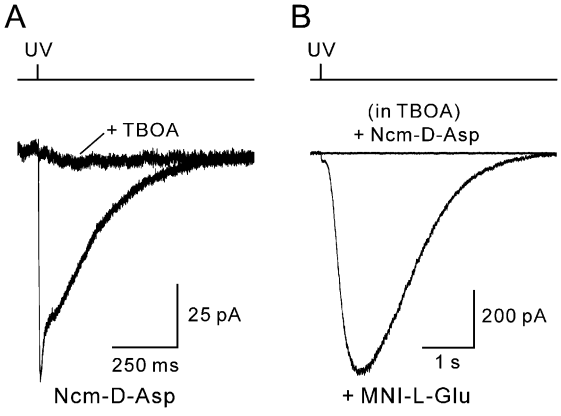

Fig. 5. Photolysis of Ncm-D-aspartate activates glutamate transporter currents but not mGluR currents or kainate receptor currents in cerebellar Purkinje cells. (A) Inward currents recorded from a Purkinje cell in response to photolysis of Ncm-D-aspartate (500 μM, 100 μm spot), in the absence and presence of TBOA (200 μM). (B) Comparison of the response of a Purkinje cell to photolysis of MNI-L-glutamate (500 μM) and Ncm-D-aspartate (500 μM) in the presence of TBOA (200 μM). All currents were recorded at −65 mV in the presence of SR 95531 (5 μM), picrotoxin (100 μM), *R,S*-CPP (10 μM) and NBQX (15 μM).

positive charges (Auger and Attwell, 2000; Huang et al., 2004a; Otis and Jahr, 1998), these results suggest that the photolysis-evoked responses reflect the cycling of 3.0×10^7 EAAT4 transporters. A similar number of transporters (2.6×10^7) were activated by photolysis of MNI-D-aspartate (500 μM) (Huang et al., 2005).

Purkinje cells express AMPA, kainate, and metabotropic glutamate receptors (mGluR1), providing an opportunity to examine whether D-aspartate released through photolysis is capable of activating these receptors. To determine whether the photo-released D-aspartate activates kainate receptors and mGluRs we compared the response of Purkinje cells with the photolysis of Ncm-D-aspartate (500 μM) and MNI-L-glutamate (500 μM). When recordings were performed in the presence of TBOA to block glutamate uptake (and antagonists of AMPA and $GABA_A$ receptors, and TTX), photolysis of MNI-L-glutamate produced a large (−500 to −1600 pA), slowly activating inward current in Purkinje cells (Fig. 5B), which was blocked by the mGluR1 antagonist LY 367385 (100 μM) (Huang et al., 2005). However, this slow inward current was not observed in response to photolysis of Ncm-D-aspartate in the presence of TBOA ($n = 3/3$ cells) (Fig. 5B), indicating that the released D-aspartate did not activate mGluR1. Notably, a small (~10 pA) rapidly activating inward current was observed in response to photolysis of MNI-L-glutamate (in the presence of 25 μM NBQX and TBOA), but not Ncm-D-aspartate (see Fig. 5B). This small current presumably results from the activation of GluR5 containing kainate receptors (Huang et al., 2004a). Although release of D-aspartate under these conditions did not result in activation of kainate receptors, some kainate receptors were blocked by NBQX in these experiments. To more stringently test whether photolysis of Ncm-D-aspartate activates these receptors, we repeated these experiments in the presence of GYKI 53655 (10 μM), a selective antagonist of AMPA receptors. Photolysis-evoked responses under these conditions were inhibited by 84.0 ± 0.8% of 200 μM TBOA, similar to the inhibition observed with NBQX ($P = 0.21$). The comparable inhibition by TBOA in these two experiments indicates that D-aspartate did not activate kainate receptors. Together, these results show that D-aspartate can be used as a selective agonist of glutamate transporters in Purkinje neurons.

3.5. NMDA receptor activation induced by photolysis of Ncm-D-aspartate

D-Aspartate is an effective ligand for NMDA receptors ($EC_{50} \cong 10$ μM) (Olverman et al., 1988), but has no appreciable activity at AMPA receptors, suggesting that Ncm-D-aspartate could be used to selectively activate NMDA receptors in neurons. To address this possibility, we measured the response of CA1 pyramidal neurons to photolysis of Ncm-D-aspartate. In the absence of antagonists of glutamate receptors and transporters, photolysis of Ncm-D-aspartate produced an inward current when pyramidal neurons were held at −20 mV (Fig. 6A). The current-to-voltage relationship of this response reversed near 0 mV and contained an area of negative slope conductance ($n = 4$) (Fig. 6B), characteristic of responses mediated by NMDA receptors. These currents were blocked by *R,S*-CPP (10 μM) and MK-801 (50 μM) ($n = 4$) (Fig. 6B), indicating that the D-aspartate released by photolysis of Ncm-D-aspartate activated NMDA but not AMPA receptors in these pyramidal neurons. Glutamate transporter-mediated currents were not detected in these neurons, presumably due to the low level of expression of EAAC1 (Bergles and Jahr, 1998; Danbolt, 2001).

Ncm-D-aspartate (1 mM) did not induce an outward current in neurons held at 30 mV ($n = 7$), indicating that Ncm-D-aspartate itself does not activate NMDA receptors and the amount of free D-aspartate in the solution was undetectable. To address whether Ncm-D-aspartate acts as an antagonist of NMDA receptors, we measured D-aspartate-evoked NMDA receptor currents in the presence or absence of 1 mM Ncm-D-aspartate. Ncm-D-aspartate did not alter the amplitude ($P = 0.101$), charge transfer ($P = 0.885$), or rise ($P = 0.646$) and decay times ($P = 0.621$) of NMDA receptor currents evoked through focal application of D-aspartate (500 μM) ($n = 7$). To test whether the caging group released by photolysis alters NMDA receptor activation, we measured D-aspartate-evoked NMDA receptor currents before, during and after

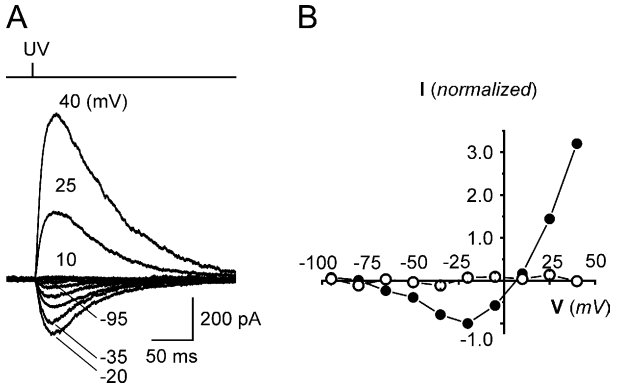

Fig. 6. Photolysis of Ncm-D-aspartate elicits NMDA receptor-mediated currents in hippocampal CA1 pyramidal neurons. (A) Response of a pyramidal neuron to photolytic release of D-aspartate recorded at different holding potentials (as indicated). The ACSF contained 1 μM TTX, and responses were recorded with a CsMeS-based internal solution. (B) Plot of the current-voltage relationship of currents recorded from CA1 pyramidal neurons in response to photolysis of Ncm-D-aspartate under control conditions (closed circles) or in the presence of *R,S*-CPP (10 μM) and MK-801 (50 μM) (open circles). Peak amplitudes were normalized to the value recorded at $V_m = -20$ mV ($n = 4$).

photolysis of Ncm-glycine (1 mM). These experiments were performed in the continuous presence of 10 μM D-serine to ensure that the glycine site of the NMDA receptor was fully occupied. As shown in Fig. 7C and D, photolysis of Ncm-glycine did not alter the amplitude or kinetics of D-aspartate evoked NMDA receptor currents ($n = 6$). These data indicate that neither Ncm-D-aspartate nor the photolyzed caging group has agonist or antagonist activity at NMDA receptors; yet Ncm-D-aspartate can be rapidly photolyzed by UV light in brain slices to release free D-aspartate to induce the selective activation of NMDA receptors in neuronal membranes.

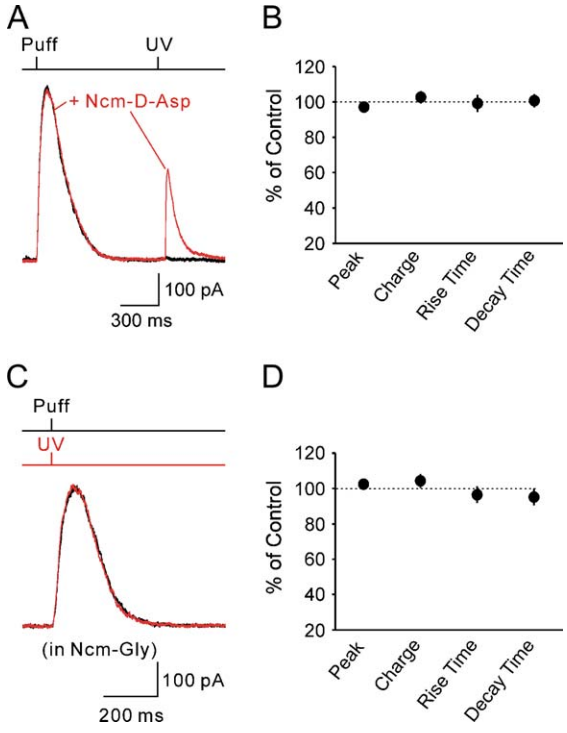

Fig. 7. Neither Ncm-D-aspartate nor the photolyzed Ncm caging group antagonize NMDA receptors. (A) NMDA receptor currents recorded at $V_m = 30$ mV in response to local pressure application of D-aspartate (500 μM; 5 ms pressure pulse) in the absence (black trace) and presence (red trace) of Ncm-D-aspartate (1 mM). A 1 ms UV flash was applied at the end of the recording to demonstrate the presence of the caged compound. (B) Grouped data showing the change in peak amplitude, charge transfer, 10–90% rise time and 90–50% decay time of NMDA receptor currents elicited through pressure application of D-aspartate, recorded in the absence and presence of 1 mM Ncm-D-aspartate ($n = 7$). (C) NMDA receptor currents evoked in a hippocampal CA1 pyramidal neuron by local pressure application of D-aspartate (500 μM; 5 ms pressure pulse), in the absence (black trace) and presence (red trace) of the UV flash (1 ms) to uncage Ncm-glycine (1 mM). (D) Grouped data showing the change in peak amplitude, charge transfer, 10–90% rise time and 90–50% decay time of puffer-evoked NMDA receptor currents recorded in the absence and presence of the photolyzed Ncm caging group ($n = 6$). All recordings were made in the presence of D-serine (10 μM) and TTX (1 μM). Pyramidal neurons were voltage-clamped at 30 mV with a CsMeS-based internal solution.

4. Discussion

In this study we describe the synthesis and physiological characterization of Ncm-D-aspartate, a novel caged analogue of D-aspartate. This compound underwent rapid photolysis upon exposure to UV light, yielding free D-aspartate at a concentration sufficient to allow rapid activation of NMDA receptors and glutamate transporters in cells within acute brain slices. This method of inducing transporter activity in situ has substantial advantages over focal application using pressure (Bergles and Jahr, 1997). Photolysis-evoked responses were more stable, they were free from mechanical and electrical artifacts, and the concentration of D-aspartate generated within the tissue could be changed rapidly by varying the laser intensity. Prior studies have used photolysis of caged L-glutamate to induce glutamate transporter currents in semi-intact preparations (Brasnjo and Otis, 2004; Canepari et al., 2001b). However, caged versions of this endogenous neurotransmitter are of limited use in studying the interaction between receptors and transporters at synapses, because glutamate will activate both simultaneously. We found that photolysis of Ncm-D-aspartate did not result in the activation mGluRs (or AMPA/kainate receptors) in neurons, indicating that photo-release of D-aspartate can be used to selectively probe the status of glutamate transporters following activation of these synaptic receptors. In vitro studies have shown that both transporter activity and density at the cell surface can be regulated through phosphorylation by protein kinase C (Gonzalez et al., 2003; Kalandadze et al., 2002), suggesting that activation of mGluRs in perisynaptic domains may trigger changes in transport capacity. The availability of a caged substrate for glutamate transporters that does not activate mGluRs will help to define the patterns of activity required to induce local changes in transporter activity in situ.

Photo-release of D-aspartate from Ncm-D-aspartate also efficiently activated NMDA receptors, indicating that this caged compound can be used to study the properties and regulation of NMDA receptors in synaptic and extrasynaptic membranes. Recent studies indicate that NMDA receptors undergo local trafficking at synapses (Perez-Otano and Ehlers, 2004), an effect that is induced following activation of mGluRs (Snyder et al., 2001). By allowing selective activation of NMDA receptors, this caged compound could also be used to determine the kinetics of receptor internalization following mGluR activation and the spatial extent of receptor changes following synaptic stimulation. A photo-labile analogue of NMDA (β-DNB NMDA) has been developed to study the gating of NMDA receptors (Gee et al., 1999). However, because NMDA is not a substrate for glutamate transporters, clearance of this ligand will depend on diffusion alone. Thus, photo-release of

NMDA in situ is likely to trigger long-duration NMDA receptor-mediated currents, limiting temporal resolution and causing substantial receptor desensitization. The properties of Ncm-D-aspartate described here indicate that it may be more suitable than caged analogues of NMDA for examining the properties and regulation of NMDA receptors in brain slices.

The amount of free D-aspartate generated over a period of days (in the dark at 4 °C) in physiological saline containing 1 mM Ncm-D-aspartate was below the limit of detection, indicating that spontaneous hydrolysis of Ncm-D-aspartate was negligibly slow or absent in aqueous solution, as one would predict from the chemical structure. Even a small amount of free D-aspartate could alter the behavior of high affinity receptors; in the case of NMDA receptors by inducing activation, desensitization, internalization, or by creating a population of singly liganded receptors; in the case of glutamate transporters, free D-aspartate would decrease the number of transporters available for uptake and potentially induce regulatory processes prior to the desired stimulus (Poitry-Yamate et al., 2002). For this reason, Ncm-D-aspartate has significant advantages over amino acids caged with the CNB-moiety, which exhibits a high rate of spontaneous hydrolysis. Neither Ncm-D-aspartate (1 mM) nor the Ncm caging group alone influenced the activity of glutamate transporters or NMDA receptors. These properties contrast with the antagonistic effects of CNB-caged-glutamate and CNB-caged-glycine at NMDA receptors (Maier et al., 2005), NI-caged GABA at $GABA_A$ receptors, and both CNI- and NI-caged-glycine at glycine receptors (Canepari et al., 2001a). However, L-glutamate caged with the NI or the MNI moiety show a similar high stability and a comparable quantum yield (Canepari et al., 2001a; Maier et al., 2005). A recently developed caged form of D-aspartate, MNI-D-aspartate, was also shown to be highly stable in aqueous solution, biologically inert, and able to trigger the activation of glutamate transporters and NMDA receptors in brain slices upon photolysis (Huang et al., 2005). MNI-D-aspartate exhibited a higher apparent quantum yield ($Q = 0.09$) than Ncm-D-aspartate ($Q = 0.04$). Consistent with this observation, it was necessary to use about twice as much Ncm-D-aspartate to elicit a transporter current of similar amplitude. However, Ncm-D-asparate, even at this higher concentration, did not measurably alter signaling through AMPA or NMDA receptors, or act as an inhibitor of glutamate transporters. Thus, MNI- and Ncm-caged versions of D-aspartate appear equally suitable for photo-release of D-aspartate under the present conditions. Recent studies have shown that MNI-L-glutamate can be photolyzed through two-photon excitation using the output of a Ti-sapphire laser, which has allowed the functional mapping of AMPA receptors on neurons (Matsuzaki et al., 2001). However, this approach requires millimolar concentrations of MNI-L-glutamate, suggesting that Ncm-D-asparate may be less suitable for studies that involve two-photon uncaging. The development of Ncm-D-aspartate as a new photo-labile form of D-aspartate suitable for triggering rapid activation of receptors and transporters within intact tissue will aid the study of the regulation of these proteins in their native membranes.

Acknowledgements

Supported by the NIH NS44564 (DEB) and GM56481 (JPYK) and the Robert Packard Center for ALS Research at Johns Hopkins (DEB). D.E.B. is an Alfred P. Sloan Research Fellow.

Appendix A. Supplementary material

Supplementary material for this manuscript can be downloaded at doi: 10.1016/j.neuropharm.2005.07.018.

References

Arnth-Jensen, N., Jabaudon, D., Scanziani, M., 2002. Cooperation between independent hippocampal synapses is controlled by glutamate uptake. Nat. Neurosci. 5, 325–331.

Arriza, J.L., et al., 1994. Functional comparisons of three glutamate transporter subtypes cloned from human motor cortex. J. Neurosci. 14, 5559–5569.

Asztely, F., Erdemli, G., Kullmann, D.M., 1997. Extrasynaptic glutamate spillover in the hippocampus: dependence on temperature and the role of active glutamate uptake. Neuron 18, 281–293.

Auger, C., Attwell, D., 2000. Fast removal of synaptic glutamate by postsynaptic transporters. Neuron 28, 547–558.

Bergles, D.E., Jahr, C.E., 1997. Synaptic activation of glutamate transporters in hippocampal astrocytes. Neuron 19, 1297–1308.

Bergles, D.E., Jahr, C.E., 1998. Glial contribution to glutamate uptake at Schaffer collateral-commissural synapses in the hippocampus. J. Neurosci. 18, 7709–7716.

Bergles, D.E., Tzingounis, A.V., Jahr, C.E., 2002. Comparison of coupled and uncoupled currents during glutamate uptake by GLT-1 transporters. J. Neurosci. 22, 10153–10162.

Brasnjo, G., Otis, T.S., 2001. Neuronal glutamate transporters control activation of postsynaptic metabotropic glutamate receptors and influence cerebellar long-term depression. Neuron 31, 607–616.

Brasnjo, G., Otis, T.S., 2004. Isolation of glutamate transport-coupled charge flux and estimation of glutamate uptake at the climbing fiber-Purkinje cell synapse. Proc. Natl. Acad. Sci. U S A 101, 6273–6278.

Canepari, M., Nelson, L., Papageorgiou, G., Corrie, J.E., Ogden, D., 2001a. Photochemical and pharmacological evaluation of 7-nitroindolinyl-and 4-methoxy-7-nitroindolinyl-amino acids as novel, fast caged neurotransmitters. J. Neurosci. Methods 112, 29–42.

Canepari, M., Papageorgiou, G., Corrie, J.E., Watkins, C., Ogden, D., 2001b. The conductance underlying the parallel fibre slow EPSP in rat cerebellar Purkinje neurones studied with photolytic release of l-glutamate. J. Physiol. 533, 765–772.

Carter, A.G., Regehr, W.G., 2000. Prolonged synaptic currents and glutamate spillover at the parallel fiber to stellate cell synapse. J. Neurosci. 20, 4423–4434.

Clark, B.A., Cull-Candy, S.G., 2002. Activity-dependent recruitment of extrasynaptic NMDA receptor activation at an AMPA receptor-only synapse. J. Neurosci. 22, 4428–4436.

Danbolt, N.C., 2001. Glutamate uptake. Prog. Neurobiol. 65, 1–105.

de Mayo, P., Shizuka, H., 1976. Measurements of reaction quantum yields. In: Ware, W.R. (Ed.), Creation and Detection of Excited States, vol. 4. Marcel Dekker, Inc., New York, pp. 139–215.

Delaney, A.J., Jahr, C.E., 2002. Kainate receptors differentially regulate release at two parallel fiber synapses. Neuron 36, 475–482.

Diamond, J.S., 2001. Neuronal glutamate transporters limit activation of NMDA receptors by neurotransmitter spillover on CA1 pyramidal cells. J. Neurosci. 21, 8328–8338.

Fairman, W.A., Vandenberg, R.J., Arriza, J.L., Kavanaugh, M.P., Amara, S.G., 1995. An excitatory amino-acid transporter with properties of a ligand-gated chloride channel. Nature 375, 599–603.

Gee, K.R., Niu, L., Schaper, K., Jayaraman, V., Hess, G.P., 1999. Synthesis and photochemistry of a photolabile precursor of *N*-methyl-D-aspartate (NMDA) that is photolyzed in the microsecond time region and is suitable for chemical kinetic investigations of the NMDA receptor. Biochemistry 38, 3140–3147.

Gonzalez, M.I., Bannerman, P.G., Robinson, M.B., 2003. Phorbol myristate acetate-dependent interaction of protein kinase C alpha and the neuronal glutamate transporter EAAC1. J. Neurosci. 23, 5589–5593.

Grewer, C., Madani Mobarekeh, S.A., Watzke, N., Rauen, T., Schaper, K., 2001. Substrate translocation kinetics of excitatory amino acid carrier 1 probed with laser-pulse photolysis of a new photolabile precursor of D-aspartic acid. Biochemistry 40, 232–240.

Grewer, C., Watzke, N., Wiessner, M., Rauen, T., 2000. Glutamate translocation of the neuronal glutamate transporter EAAC1 occurs within milliseconds. Proc. Natl. Acad. Sci. U S A 97, 9706–9711.

Grunewald, M., Kanner, B., 1995. Conformational changes monitored on the glutamate transporter GLT-1 indicate the existence of two neurotransmitter-bound states. J. Biol. Chem. 270, 17017–17024.

Hatchard, C.G., Parker, C.A., 1956. A new sensitive chemical actinometer. II. Potassium ferrioxalate as a standard chemical actinometer. Proc. Roy. Soc. London, Ser. A. 235, 518–536.

Huang, Y., Sinha, S., Fedoryak, O., Ellis-Davies, G., Bergles, D., 2005. Synthesis and characterization of 4-methoxy-7-nitroindolinyl-D-aspartate, a caged compound for selective activation of glutamate transporters and *N*-methyl-D-aspartate receptors in brain tissue. Biochemistry [Published online, Feb. 12, 2005].

Huang, Y.H., Dykes-Hoberg, M., Tanaka, K., Rothstein, J.D., Bergles, D.E., 2004a. Climbing fiber activation of EAAT4 transporters and kainate receptors in cerebellar Purkinje cells. J. Neurosci. 24, 103–111.

Huang, Y.H., Sinha, S.R., Tanaka, K., Rothstein, J.D., Bergles, D.E., 2004b. Astrocyte glutamate transporters regulate metabotropic glutamate receptor-mediated excitation of hippocampal interneurons. J. Neurosci. 24, 4551–4559.

Kalandadze, A., Wu, Y., Robinson, M.B., 2002. Protein kinase C activation decreases cell surface expression of the GLT-1 subtype of glutamate transporter. Requirement of a carboxyl-terminal domain and partial dependence on serine 486. J. Biol. Chem. 277, 45741–45750.

Lehre, K.P., Danbolt, N.C., 1998. The number of glutamate transporter subtype molecules at glutamatergic synapses: chemical and stereological quantification in young adult rat brain. J. Neurosci. 18, 8751–8757.

Lehre, K.P., Levy, L.M., Ottersen, O.P., Storm-Mathisen, J., Danbolt, N.C., 1995. Differential expression of two glial glutamate transporters in the rat brain: quantitative and immunocytochemical observations. J. Neurosci. 15, 1835–1853.

Maier, W., Corrie, J.E., Papageorgiou, G., Laube, B., Grewer, C., 2005. Comparative analysis of inhibitory effects of caged ligands for the NMDA receptor. J. Neurosci. Methods 142, 1–9.

Matsuzaki, M., et al., 2001. Dendritic spine geometry is critical for AMPA receptor expression in hippocampal CA1 pyramidal neurons. Nat. Neurosci. 4, 1086–1092.

McCray, J.A., Trentham, D.R., 1989. Properties and uses of photoreactive caged compounds. Annu. Rev. Biophys. Biophys. Chem. 18, 239–270.

Oliet, S.H.R., Piet, R., Poulain, D.A., 2001. Control of glutamate clearance and synaptic efficacy by glial coverage of neurons. Science 292, 923–926.

Olverman, H.J., Jones, A.W., Mewett, K.N., Watkins, J.C., 1988. Structure/activity relations of *N*-methyl-D-aspartate receptor ligands as studied by their inhibition of [3H]D-2-amino-5-phosphonopentanoic acid binding in rat brain membranes. Neuroscience 26, 17–31.

Otis, T.S., Jahr, C.E., 1998. Anion currents and predicted glutamate flux through a neuronal glutamate transporter. J. Neurosci. 18, 7099–7110.

Otis, T.S., Kavanaugh, M.P., Jahr, C.E., 1997. Postsynaptic glutamate transport at the climbing fiber-Purkinje cell synapse. Science 277, 1515–1518.

Perez-Otano, I., Ehlers, M.D., 2004. Learning from NMDA receptor trafficking: clues to the development and maturation of glutamatergic synapses. Neurosignals 13, 175–189.

Pettit, D.L., Wang, S.S., Gee, K.R., Augustine, G.J., 1997. Chemical two-photon uncaging: a novel approach to mapping glutamate receptors. Neuron 19, 465–471.

Poitry-Yamate, C.L., Vutskits, L., Rauen, T., 2002. Neuronal-induced and glutamate-dependent activation of glial glutamate transporter function. J. Neurochem. 82, 987–997.

Rothstein, J.D., et al., 1994. Localization of neuronal and glial glutamate transporters. Neuron 13, 713–725.

Schupp, H., Wong, W.K., Schnabel, W., 1987. Mechanistic studies of the photorearrangement of *o*-nitrobenzyl esters. J. Photochem. 36, 85–97.

Shigeri, Y., et al., 2001. Effects of *threo*-beta-hydroxyaspartate derivatives on excitatory amino acid transporters (EAAT4 and EAAT5). J. Neurochem. 79, 297–302.

Shimamoto, K., et al., 1998. DL-*threo*-beta-benzyloxyaspartate, a potent blocker of excitatory amino acid transporters. Mol. Pharmacol. 53, 195–201.

Snyder, E.M., et al., 2001. Internalization of ionotropic glutamate receptors in response to mGluR activation. Nat. Neurosci. 4, 1079–1085.

Wadiche, J.I., Arriza, J.L., Amara, S.G., Kavanaugh, M.P., 1995. Kinetics of a human glutamate transporter. Neuron 14, 1019–1027.

Walker, J.W., Reid, G.P., McCray, J.A., Trentham, D.R., 1988. Photolabile 1-(2-nitrophenyl)ethyl phosphate esters of adenine nucleotide analogs. Synthesis and mechanism of photolysis. J. Am. Chem. Soc. 110, 7170–7177.

Walker, J.W., Reid, G.P., Trentham, D.R., 1989. Synthesis and properties of caged nucleotides. Meth. Enzymol. 172, 288–301.

Yip, R.D., Sharma, D.K., Giasson, R., Gravel, D., 1985. Photochemistry of the *o*-nitrobenzyl system in solution: evidence for singlet-state intramolecular hydrogen abstraction. J. Phys. Chem. 89, 5328–5330.

Yip, R.W., Wen, Y.X., Gravel, D., Giasson, R., Sharma, D.K., 1991. Photochemistry of the *o*-nitrobenzyl system in solution: identification of the biradical intermediate in the intramolecular rearrangement. J. Phys. Chem. 95, 6078–6081.

Zerangue, N., Kavanaugh, M.P., 1996. Flux coupling in a neuronal glutamate transporter. Nature 383, 634–637.

Zhu, Q.Q., Schnabel, W., Schupp, H., 1987. Formation and decay of nitronic acid in the photorearrangement of *o*-nitrobenzyl esters. J. Photochem. 39, 317–332.